

Institut für Plasmaphysik  
KERNFORSCHUNGSANLAGE JÜLICH  
des Landes Nordrhein-Westfalen

MEASUREMENTS OF ION ENERGY  
DISTRIBUTION ON A PLASMA GUN

by

W. Bieger, D. Dorn,  
P. Noll and H. Tuczec

Jül - 22 - PP

Oktober 1961

Als Manuskript gedruckt





Berichte der Kernforschungsanlage Jülich – Nr. 22

Institut für Plasmaphysik Jülich – 22 – PP

Dok.: PLASMA-PROPERTIES \* DK 537.525.1

Zu beziehen durch: ZENTRALBIBLIOTHEK der Kernforschungsanlage Jülich,  
Jülich, Bundesrepublik Deutschland

# MEASUREMENTS OF ION ENERGY DISTRIBUTION ON A PLASMA GUN

by

W. Bieger, D. Dorn,

P. Noll and H. Tuczek

# MEASUREMENTS OF ION ENERGY DISTRIBUTION ON A PLASMA GUN

by

W. Bieger, D. Dorn, P. Noll and H. Tucek\*

Institut für Plasmaphysik der Kernforschungsanlage Jülich / Germany

## ABSTRACT

Time resolved energy distributions of ions of the plasma ejected by a hydromagnetic gun have been measured by a retarding potential spectrometer. Three pulses corresponding to different periods of origin are observed and analyzed. The longitudinal energy of the ions is in the range from 200 eV to about 1 keV, the ion temperature being of the order of 1 eV. The influence of diaphragms and the retarding field on the plasma is studied and discussed.

## 1. INTRODUCTION

This paper gives a report on measurements with a hydromagnetic plasma gun, which are being performed to prepare the injection of plasma into different magnetic field configurations. A number of methods are known for the determination of physical properties of accelerated plasmas (1, 2) .

The retarding potential method, described in this paper, gives a time resolved energy distribution of the ejected plasma. The basic-problem

\*Presented at the Fifth International Conference on Ionisation Phenomena in Gases, Munich 1961.

To be published in the proceedings of this conference.



hereby is to avoid disturbance of the distribution to be measured by the measuring apparatus itself. Errors may result from interaction with diaphragms, used to limit the plasma jet in space, as well as from the electric field, caused by charge separation in the retarding field. These fields may be of the same order of magnitude, when the plasma density is too high.

In order to reduce the initially high density by lateral diffusion, the plasma has to cover a large distance to the measuring apparatus. In addition, this large distance allows to determine the energy of the ions by time of flight whereby the retarding potential method can be checked. This is possible, if the ions do not interact strongly on their way. The fact that the temporal and spatial origin of the ejected plasma is not known exactly limits the accuracy. The energy distribution is obtained in the case of the retarding potential method by superposing several discharges, the fluctuations of which reduce again the accuracy of measurement and the possibility to compare with the time of flight method.

It is planned to use a magnetic spectrograph, differential results may then be obtained from a single discharge.

## 2. EXPERIMENTAL ARRANGEMENT

Fig. 1 shows a schematic sketch of the apparatus. Through a quick-acting electromagnetic valve, a pulse of  $H_2$  gas enters the evacuated system during a time interval of a few 100  $\mu s$ . The vacuum chamber consists of a glass-pipe, 2 meters in length and with a diameter of 10 cm. The gas is preionized by a pulsed electrodeless ring discharge near the entrance of the conical compression coil (cone angle  $90^\circ$ ) and is then compressed and axially accelerated into the vacuum by the oscillating magnetic field. This field is induced by the discharge of a bank of  $10 \times 0.5 \mu F$  low inductance condensers charged to a voltage of 24 kV. Each capacitor is separately switched by a triggered spark gap. The

ringing period of the discharge is  $3.2 \mu\text{s}$ . After having covered a distance of 2 m, the plasma enters a system of 2 to 3 diaphragms, each with a diameter of 1 mm and an overall distance of about 30 cm. The retarding potential is applied to a grid with 1 cm diameter and about 50 meshes per  $\text{mm}^2$ . The length of the retarding field is 4 mm, the distance between the grid and the diaphragm, separating the retarding field from a post-accelerating field, is 9 mm.

This diaphragm consists of a double-grid with a diameter of about 3 cm. Having passed this grid, the ions are post-accelerated in a field perpendicular to the axis of the plasma jet onto a plastic scintillator. For this purpose a grid covering the scintillator is charged to a potential of - 30 kV. The resulting photons are led along a quartz light pipe out of the vacuum system and are detected by a photomultiplier tube. The output signals and their time integral are recorded as a function of the retarding potential by an oscilloscope.

At two positions along the glass pipe the light emitted by the plasma is observed normal to the axis by photomultiplier tubes. In front of the first diaphragm the appearance of the plasma is observed by a 8 mm-microwave interferometer. Kerr-cell photographs of the discharge in the coil show the ejection of the plasma in different half cycles of the discharge. Measurements with magnetic probes and pick-up coils around the pipe are performed in order to observe diamagnetic properties of the plasma and trapped magnetic fields. A magnetic guide field along the tube ( 10 kGauss maximum with a ringing period of 2 ms) may be switched on for this purpose.

### 3. MEASUREMENTS WITH THE RETARDING POTENTIAL METHOD

Fig. 2 shows the behaviour of the ion pulses with increasing retarding potential. Three subsequent components may be distinguished, with a duration short compared with the time of flight of the ions, vanishing at different but definite retarding potentials. The pulses, in particular the two first, decay from their rear side, as indicated in Fig. 2.

The ions, corresponding to these pulse rear sides, are just able to overcome the retarding potential. Time of flight analysis of these ions shows that the first component with an average energy of 315 eV originates at the end of the first half cycle, the second component with an average of 215 eV in the second half cycle just after the current maximum. This is confirmed by Kerr-cell photographs which show that the main plasma emission occurs in the second half cycle, when the trapped field is antiparallel to the compression field. The third component with an energy of 1.1 keV seems to originate in the 6th half cycle. This indicates that caused by the strong emission in the second half cycle, discharge conditions inside the coil have changed and further emission of plasma is possible only after a number of ionizing half cycles. This is verified by measurements of the light emission by photomultiplier tubes.

Fig. 3 shows the dependence of the time integrated ion signals on the retarding potential. Fluctuations of the discharge make it impossible to determine the exact form of the energy distribution of the different components by analysing the slopes. But an upper limit  $E_{\max}$  and a lower limit  $E_{\min}$  of the energy of the ions can be determined by a linear approximation of these slopes, especially for the second component. Thereby assuming a rectangular energy distribution between  $E_{\min}$  and  $E_{\max}$ , the average ion energy of each component in its center of mass system is

$$\bar{E}_s = \frac{1}{24} \cdot \frac{(E_{\max} - E_{\min})^2}{E_{\max} + E_{\min}}.$$

The following table shows these energy values for the different components:

component	1	2	3
maximum energy $E_{\max}$	360 eV	260 eV	1300 eV
minimum energy $E_{\min}$	270 eV	170 eV	850 eV
in the center of mass system			
mean energy $E_s$	0.5 eV	1 eV	4 eV
intensity	4 %	71 %	25 %
origin	first halfcycle	second halfcycle	sixth halfcycle

The intensity of these pulses is strongly dependent on the contamination of the plasma. If the absorbed gas at the glass surface is removed by a number of discharges, the first and the third component of the ion pulses are scarcely detectable.

#### 4. CAUSES OF ERRORS

In order to estimate the influence of the diaphragms, limiting the plasma jet, on the accuracy of the retarding potential method, the diameter and the distance between the diaphragms were varied.

A comparison of the ion signals shows an influence greater than should be expected by geometric diminution. The observed reduction in plasma density between the diaphragms corresponds to an angular dispersion of about  $1^\circ$  if one assumes a homogeneous radial density distribution.

Fig. 4 shows the dependence of the ion intensity on the time interval  $\Delta t$  between the opening of the valve and the triggering of the main discharge, the distances between the second and the third diaphragm being 80 mm (curve I) and 140 mm (curve II) respectively. With decreasing  $\Delta t$  the gas density in the compression coil decreases, while the velocity of the accelerated plasma increases.

The quotient of the intensity of curve I over the intensity of curve II indicates, that the angular dispersion of the plasma due to the interaction with the diaphragm depends on the axial velocity as well as on the density of the plasma in front of the diaphragm. The ratio of the Debye-shielding distance to the diameter of the diaphragm should be the important parameter for this dependence.

Fluctuations of the density and the electron temperature of the plasma may therefore lead to false energy distributions. By comparison of the ion signals for different positions of the diaphragm-system the perturbation can be estimated. In the cases discussed in this paper, this check gave at the utmost a change in the relative intensities of the components, but no change in the shape of the single components.



Further errors in the measurement of the energy distribution may result from the electric field created by charge separation in the retarding field. A positive space-charge in front of the retarding potential grid may cause the ions to be deflected, although they have an energy large enough to overcome the potential barrier. This effect depends on the ion density in the retarding field region.

Measurements with a greater distance between the grid of the retarding field and a 3 mm diaphragm, separating this field from the subsequent accelerating field, give the order of magnitude of this effect. The integral curve, corresponding to the curve in fig. 3, then shows an increasing dispersion with increasing retarding potential, beginning already at relatively low values. Assuming a homogeneous density of the jet behind the grid, neglecting an additional broadening of the jet by the mutual repulsion of the ions, and neglecting the inhomogeneity of the field, radial energies of the order of 1 eV are obtained for ions, which are just able to overcome the retarding potential. Taking into consideration ions which already have been slowed down in the retarding field, an estimate of the electrostatic repulsion in this field gives the same order of magnitude for the radial divergence of the jet.

An upper limit of the energy broadening gives fig. 2. By increasing the retarding potential the pulses decay in an interval of 0.3 to 0.5  $\mu\text{sec}$ , corresponding to an energy interval  $\leq 20$  eV. This should be caused mainly by the emission of the plasma during a corresponding time interval of the discharge with a finite energy distribution. The contribution of the energy broadening due to impacts in the initial, dense plasma should be negligible in the case of no axial guide field applied, as the density of the plasma then decreases rapidly during its axial motion.

## 5. INFLUENCE OF DISCHARGE PARAMETERS

The magnitude of the ion signals gives a rough estimate of the number of ions. The plasma emitted in the second half cycle contains about  $10^{16}$  ions.

In this estimate approximate values are assumed for the attenuation by the diaphragms, the grids, and the scintillator. Furthermore, it is assumed that about 90 % of the ions are neutralized before they reach the retarding field. The plasma density just in front of the first diaphragm is about  $10^{11} \text{ cm}^{-3}$ . This is verified by micro-wave measurements at this point, which show that the microwave signal appears just after the scintillator signal, probably due to an increase of density by reflected particles from the diaphragm.

The intensity and the average energy of the ion pulses strongly depend on the initial distribution of the gas density in the discharge coil and on the preionisation of the gas. The density distribution may be changed both by varying the time interval  $\Delta t$  between the opening of the valve and the triggering of the discharge or by varying the pressure in the valve itself. As a function of  $\Delta t$  the intensity of the ion signals has a maximum (fig.4). When  $\Delta t$  is small, the ionisation and therefore the quantity of the accelerated plasma is small, too. If on the other hand  $\Delta t$  is large, a greater quantity of gas has already streamed into the pipe in front of the discharge coil so that the ejected plasma interacts with gas and diffuses towards the walls.

Fig. 5 shows, that the average ion energy increases when  $\Delta t$  decreases, i.e. when the initial gas density decreases. The influence of the pressure in the valve on the discharge has not been studied systematically. Preliminary measurements indicate, that a high pressure (3 atm) and low  $\Delta t$  ion pulses may origin in the first half cycle with an energy of a few keV. Without preionisation the separation of the ion signal in three components is essentially more distinct. The intensity of the signals is about four times smaller, while the average energy of the ions decreases (from 215 eV for the second component). This dependence shows that by improving the preionisation and the initial distribution of the gas density, an increase of the intensity and the ion energy of the accelerated plasma is possible.

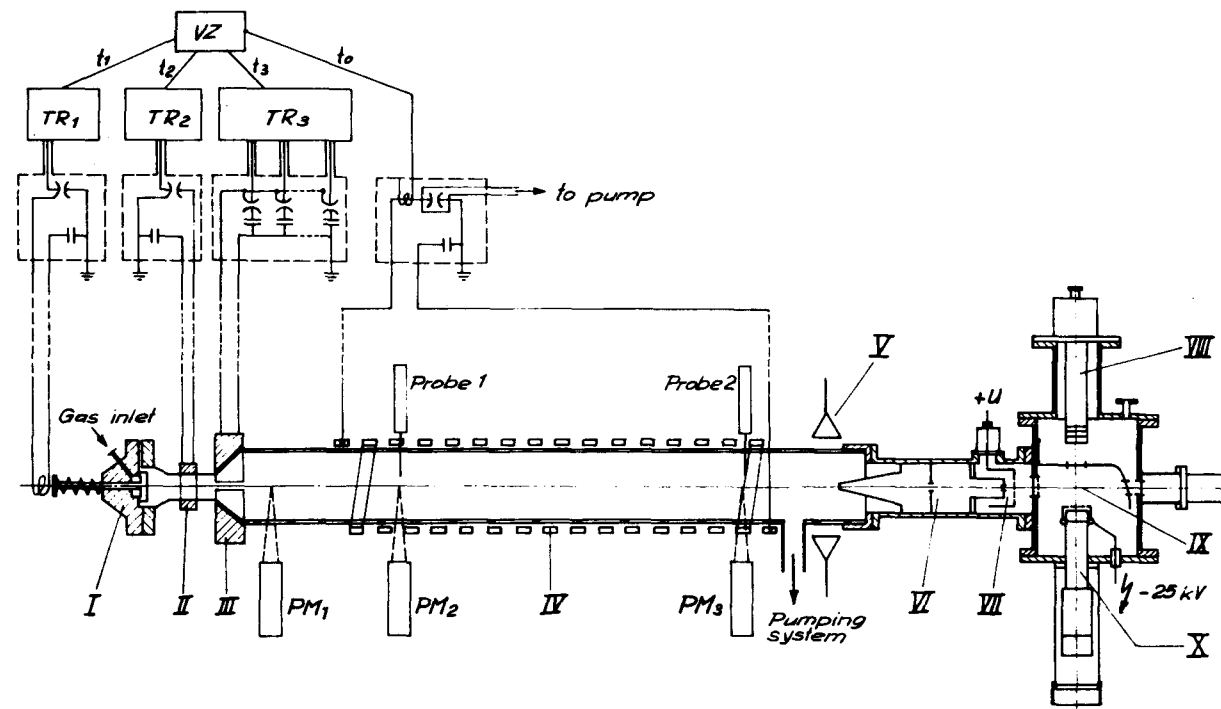
## ACKNOWLEDGEMENTS

We have to thank Prof. Fucks for his continuous interest and support. Furthermore we are indebted to Dr. H.L. Jordan and P. Gräff for helpful discussions. Especially we have to thank H. Geller and H. Gresser, who essentially took part in constructing the plasma gun, for Kerr-cell photographs and assistance in measurements. Microwave measurements of H. Beerwald are gratefully acknowledged.

## LITERATURE

1. John Marshall, in "Plasma Acceleration", S.W. Kash (ed.) Stanford 1960, p. 60
2. F. Waelbroeck, C. Leloup, J.P. Poffé, P. Evrad, et D. Veron, "Conference on Plasma Physics and Controlled Nuclear Fusion Research", Salzburg, September 1961, GN-10/103/A.
3. P.I. Richards, E.E. Hays, Rev. Sci. Instrum. 21, 99 (1950).





- |                            |                            |                                    |
|----------------------------|----------------------------|------------------------------------|
| I Fast valve               | VI Diaphragm system        |                                    |
| II Pre ionisation coil     | VII Retarding field        |                                    |
| III Compression coil       | VIII Ion source            | PM <sub>1</sub>                    |
| IV Guide field solenoid    | IX Post acceleration field | PM <sub>2</sub> } Photo multiplier |
| V Microwave-interferometer | X Scintillation detector   | PM <sub>3</sub>                    |

Fig. 1: Experimental arrangement.

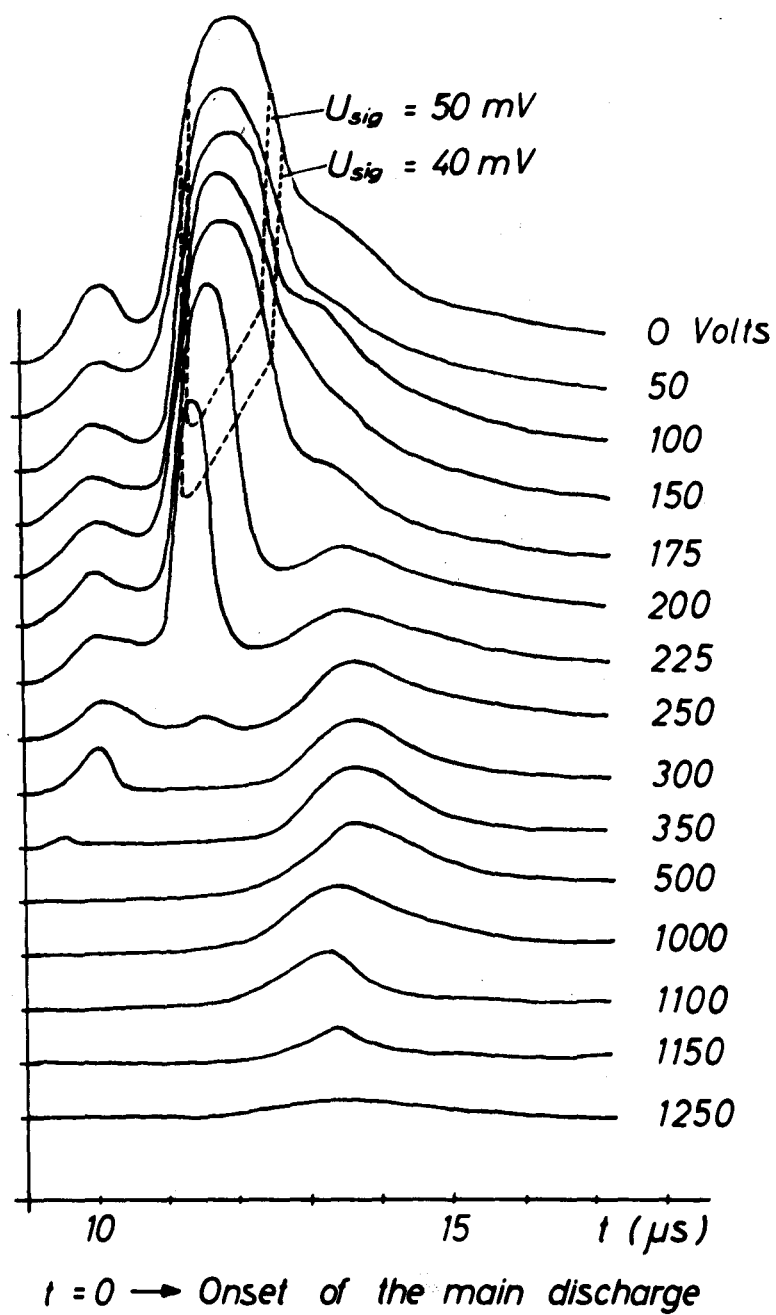


Fig. 2: Ion signal as a function of the retarding potential.

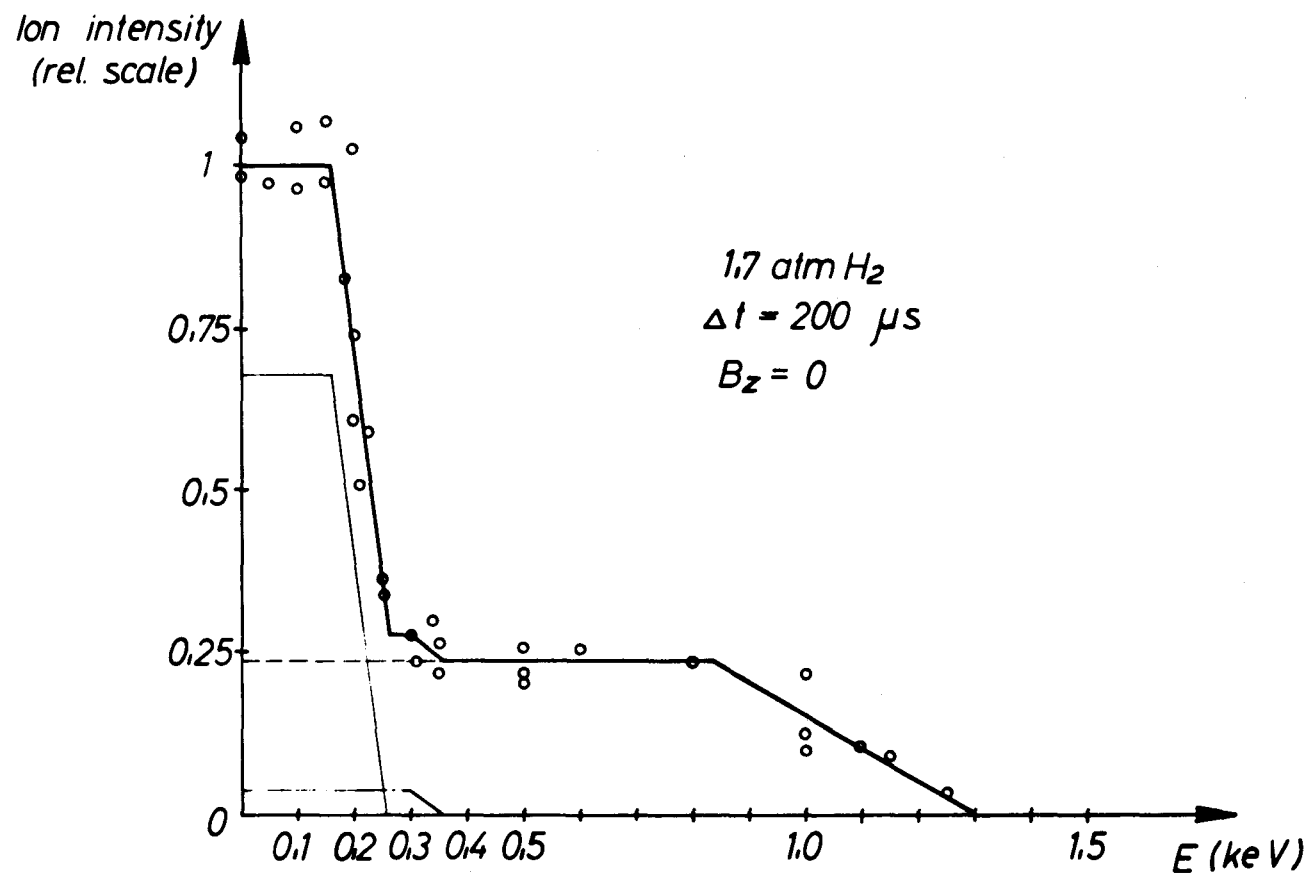


Fig. 3: Ion intensity as a function of the retarding field.



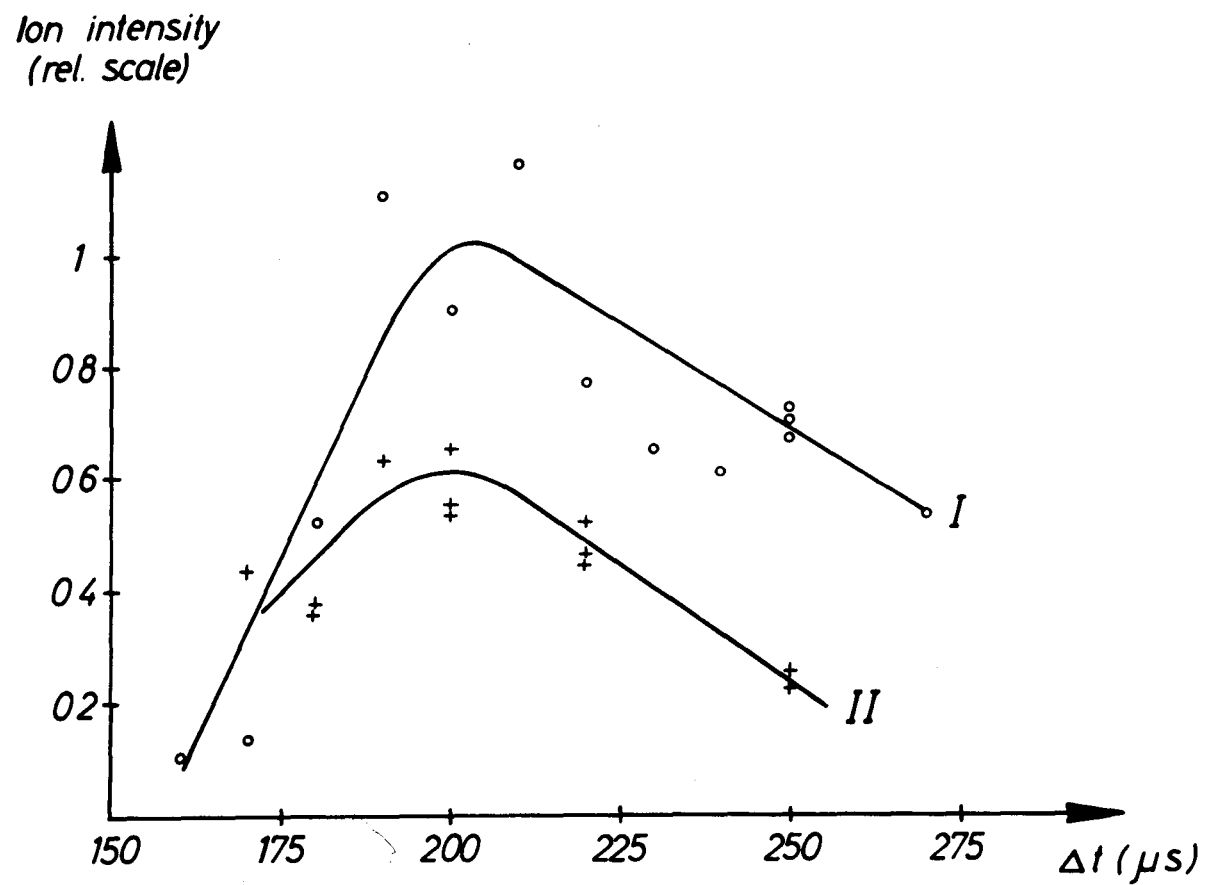


Fig. 4: Ion intensity as a function of the delay  $\Delta t$  between gas admission and firing of the main bank at different arrangements of the diaphragms.

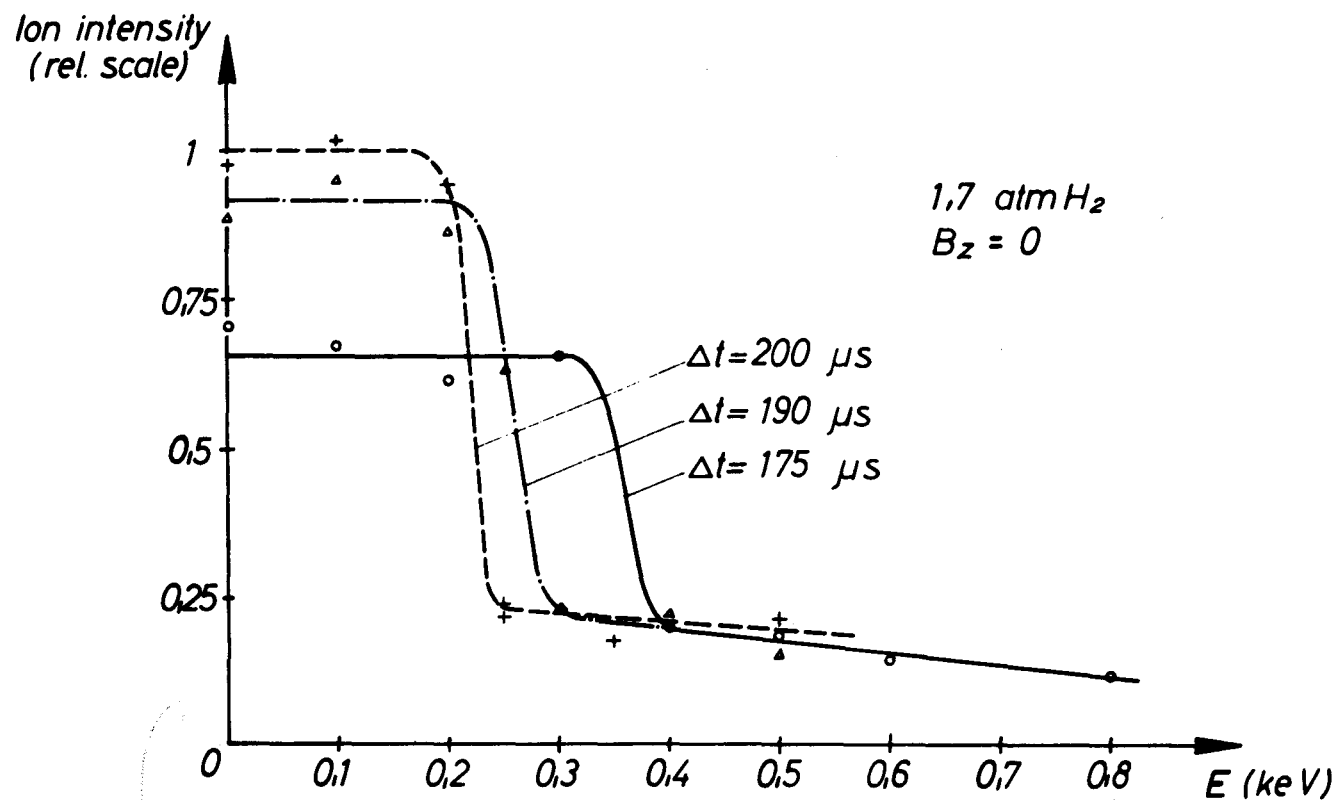


Fig. 5: Ion intensity as a function of the retarding field for various delays  $\Delta t$  between gas admission and firing of the main bank.

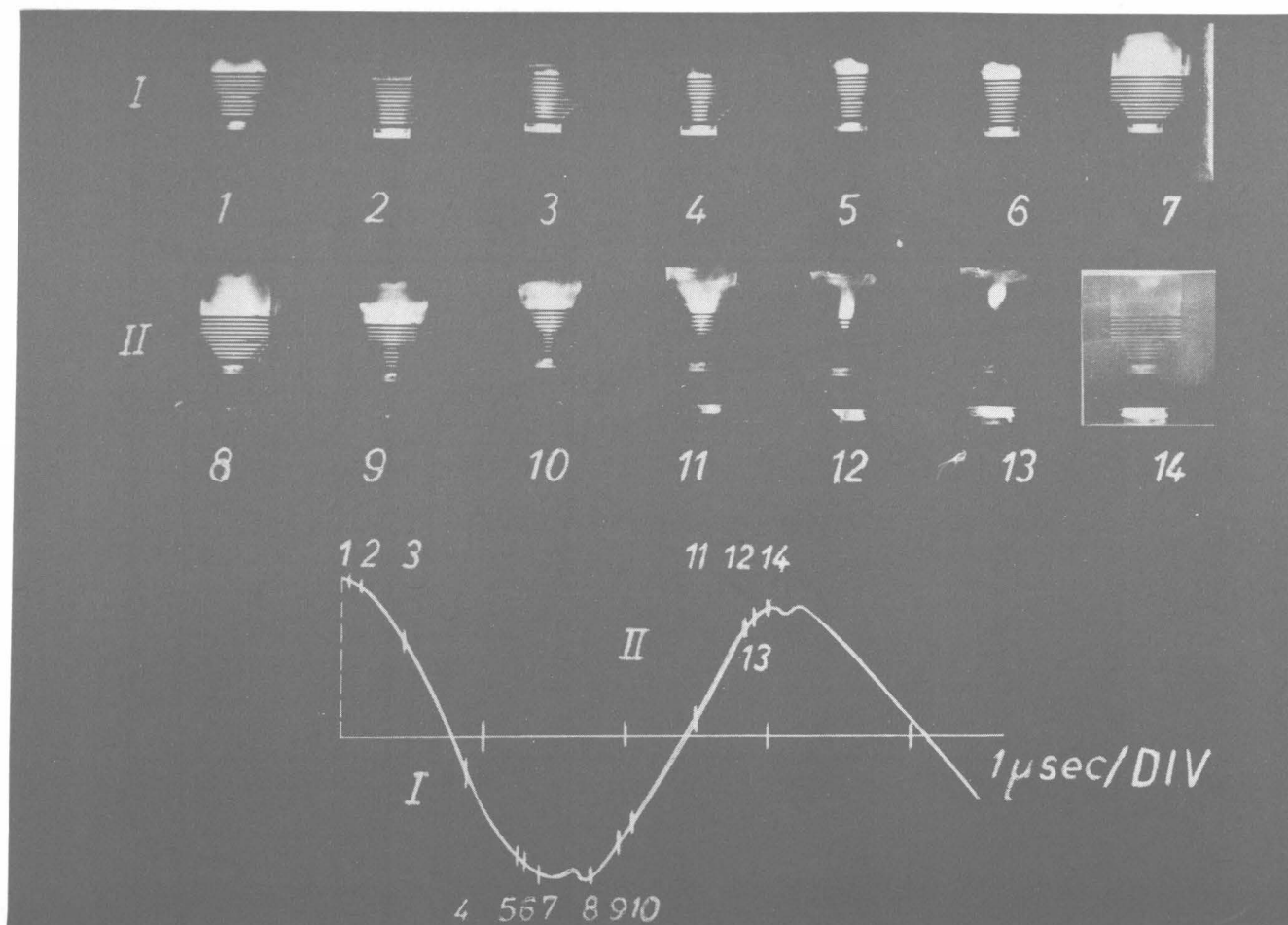


Fig. 6: Kerr cell photographs in the first and second halfcycle of the discharge. (exposure time about  $10^{-7}$  sec.)